Environmental Science & Technology

pubs.acs.org/est

Article

Biofilm Control in Flow-Through Systems Using Polyvalent Phages Delivered by Peptide-Modified M13 Coliphages with Enhanced Polysaccharide Affinity

Ruonan Sun, Pingfeng Yu,* Pengxiao Zuo, Dino Villagrán, Jacques Mathieu, and Pedro J.J. Alvarez*

Cite This: *Environ. Sci. Technol.* 2022, 56, 17177−17187

Read Online

ACCESS | Metrics & More | Article Recommendations | Supporting Information

ABSTRACT: Eradication of biofilms that may harbor pathogens in water distribution systems is an elusive goal due to limited penetration of residual disinfectants. Here, we explore the use of engineered filamentous coliphage M13 for enhanced biofilm affinity and precise delivery of lytic polyvalent phages (i.e., broad-host-range phages lysing multiple host strains after infection). To promote biofilm attachment, we modified the M13 major coat protein (pVIII) by inserting a peptide sequence with high affinity for *Pseudomonas aeruginosa* (*P. aeruginosa*) extracellular polysaccharides (commonly present on the surface of biofilms in natural and engineered systems). Additionally, we engineered the M13 tail fiber protein (pIII) to contain a peptide sequence capable of binding a specific polyvalent lytic phage. The modified M13 had 102- and 5-fold higher affinity for *P. aeruginosa*-dominated mixed-species biofilms than wildtype M13 and unconjugated polyvalent phage, respectively. When applied to a simulated water distribution system, the resulting phage conjugates achieved targeted phage delivery to the biofilm and were more effective than polyvalent phages alone in reducing live bacterial biomass (84 vs 34%) and biofilm surface coverage (81 vs 22%). Biofilm regrowth was also mitigated as high phage concentrations induced residual bacteria to downregulate genes associated with quorum sensing and extracellular polymeric substance secretion. Overall, we demonstrate that engineered M13 can enable more accurate delivery of polyvalent phages to biofilms in flow-through systems for enhanced biofilm control.

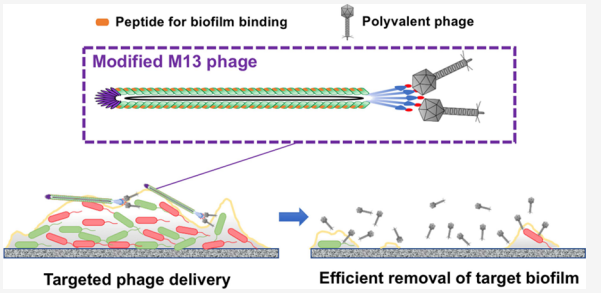

KEYWORDS: *biofilm control, polyvalent phage, phage display, phage conjugates, targeted delivery*

INTRODUCTION

Biofilms, which are complex microbial aggregates embedded in heterogeneous extracellular polymeric substrates (EPS),[1] are pervasive in water distribution systems.[2] Biofilms can harbor pathogenic microbes and accelerate infrastructure corrosion, causing a variety of health, operational, and aesthetic concerns.[3] Conventional biofilm control approaches are marginally effective or impractical, as residual chemical disinfectants do not effectively penetrate the biofilm matrix and energy-intensive mechanical devices are generally unfeasible to clean water pipes.[2,4,5] Increasing incidences of infectious diseases transmitted by drinking water[6−9] underscores the need for innovation, including bio-inspired approaches that control biofilms while avoiding collateral oxidative damage to infrastructure or the formation of carcinogenic disinfection byproducts.[2]

Phages, which are viruses that exclusively infect bacteria, are garnering significant interest as eco-friendly, self-replicating biocides for biofilm control.[10−12] Specifically, phages can propagate in and kill common biofilm-dwelling bacterial hosts, with some phages possessing depolymerases that can facilitate biofilm penetration and degradation of the EPS matrix.[13] Since phage replication is a host cell density dependent process, phage concentrations decrease rapidly when the target bacteria are eradicated, following a typical predator−prey relation and posing low potential risks.[14] Furthermore, phages with useful traits for biofilm control (e.g., high propagation within biofilm) can be isolated from common environments and enhanced by genetic manipulations.[13,15] However, phage infection of biofilms can be hindered by hydrodynamic conditions that result in short contact times, phage dilution, and off-target attachment.[16,17] Additionally, exposure to low phage concentrations as a result of inefficient delivery may hormetically stimulate biofilm growth instead of eradicating it.[18] Therefore, enhanced phage delivery is important for efficient biofilm removal in water distribution systems.

Targeting biofilms in flow-through systems with phages is challenging because the affinity of phages for biofilms (crucial

Received: September 8, 2022
Revised: November 9, 2022
Accepted: November 10, 2022
Published: November 22, 2022

for targeting biofilms in flow-through systems) is often inversely correlated with phage dispersity within biofilms (critical for phage propagation and biofilm eradication).[19,20] However, we postulate that phages with high infectivity could be conjugated with carrier phages exhibiting high biofilm affinity to achieve targeted lytic phage delivery and effective biofilm control.

Phage display is a common technique to enable high throughput screening of peptides with a strong affinity to various targets, including bacterial surfaces and biofilm matrices.[21−23] Such peptides can be displayed or immobilized onto various substrates to promote selective binding to target bacteria on biofilm surfaces.[24−26] Filamentous coliphage M13 has been extensively studied for phage display and also has capsid and tail fiber proteins, which have proven to be amenable to genetic modification.[27] Therefore, dual modification[28] of the phage M13 capsid (for biofilm recognition) and tail fibers (for polyvalent lytic phage conjugation) could enhance lytic phage delivery to biofilms in flow-through systems and facilitate phage infection of relatively abundant biofilm-dwelling bacteria. Furthermore, such phage modifications would not introduce pathogenic elements or alter the host range of M13.[27] Thus, such modifications to M13 would not be expected to alter its safety profile.

This work describes the development and application of modified M13 phages, conjugated with polyvalent lytic phages, for clearance of a simple, dual-species biofilm [*Pseudomonas aeruginosa* (*P. aeruginosa*) and *Escherichia coli* (*E. coli*)] in a flow-through system (i.e., a model water distribution pipe). *P. aeruginosa* is an opportunistic pathogen commonly present in drinking water system biofilms[29−32] and is increasingly recognized as a major agent of concern in drinking water supplies.[33−40] Additionally, *P. aeruginosa* is frequently observed to dominate multi-species biofilms in diverse environments[41−46] due to its relatively high growth rate,[41] high dispersivity,[47] inhibition of neighboring bacteria (via T6SS and toxin production),[48−50] and great ability for colonization and matrix formation.[51,52] *E. coli* ranks third in the WHO list of antibiotic-resistant "priority pathogens"[53] and could enter drinking water distribution systems (DWDS) through infiltration.[54] Short peptides with high affinity for *P. aeruginosa* were screened from a peptide library by phage display and fused onto the major coat protein (pVIII) of phage M13. Peptides with high affinity to polyvalent lytic phages were also introduced onto the tail fiber protein (pIII) of M13 to facilitate phage loading. Genome sequencing and surface characterization were conducted to verify the dual modification of M13, and conjugation with polyvalent phages was verified by fluorescent microscopic analysis. Enhanced polyvalent phage delivery and biofilm control by these phage conjugates relative to free phages were also demonstrated in proof-of-concept experiments.

MATERIALS AND METHODS

Chemicals, Bacterial Strains, and Culture Conditions. The bacterial strains used in this study included *P. aeruginosa* PAO1 (ATCC 15692) and *E. coli* NDM-1 (ATCC BAA-2452). These bacterial strains were routinely grown in Luria Bertani broth (BD Biosciences, USA) at 37 °C overnight with gentle shaking at 60 rpm. Total viable bacteria were counted by a plate assay using Difco plate count agar (BD Biosciences, USA) and expressed as colony-forming units (CFU).[10]

Reagents purchased from Millipore Sigma (USA) include N-hydroxysuccinimide (NHS), 1-ethyl-3-(3-(dimethylamino)-propyl) carbodiimide hydrochloride (EDC), vancomycin, bovine serum albumin (BSA), oligonucleotides, mutanolysin, PES filter membranes, sodium periodate, and TEXAS RED conjugated with streptavidin. Reagents from New England Biolabs (USA) include Ph.D.-7 and -12 Phage Display Peptide Library, *E. coli* ER2738, phage genome of M13KE, T4 ligase, and restriction enzymes *Eag*I, *Acc*65I, *Pst*I, and *BamH*I. Reagents from Invitrogen (USA) include proteinase K, Sodium dodecyl sulfate (SDS), biotinylated anti-M13 phage coat protein antibodies (MM05), SYBR gold, and LIVE/DEAD BacLight kit.

Isolation of Polyvalent Lytic Phages. Polyvalent lytic phages infecting both *P. aeruginosa* and *E. coli* were isolated using a modified sequential multiple-host approach from activated sludge. Briefly, amine-functionalized iron-carbide (Fe_3C-NH_2) magnetic colloidal nanoparticle clusters (CNCs) were conjugated with vancomycin (using EDC and NHS as crosslinkers) and poly(ethylene glycol) (PEG).[55,56] The modified CNCs (∼1 mg) and bacterial cells (exponential state, diluted to OD_{600} = 0.1) were conjugated by mixing for 10 min at 4 °C. The phage pool from activated sludge sequentially went through CNCs-*P. aeruginosa* and CNCs-*E. coli* complexes to obtain phages that can be adsorbed and enriched by both *P. aeruginosa* and *E. coli*. CNC-bacteria complexes enabled a more gentle and complete separation of bacteria-adsorbed phages [by using a neodymium magnet (K&J Magnetics, Grade N52, 600 gauss) to attract CNC-bacteria complexes with adsorbed phages to the bottom of the tube] than traditional centrifugation or filtration processes.[57,58] Details of phage isolation are provided in the Supporting Information (SI) as Text S1.

The polyvalent phages were propagated in *P. aeruginosa* culture overnight at 37 °C, and then the bacterial cells were removed via centrifugation (4 °C, 8000 × *g*, 8 min) followed by filtration through 0.22 μm PES filter membranes. Phages were further concentrated and purified by PEG precipitation and suspended in SM buffer prior to storage at 4 °C. Phage concentration was determined before each use by the double-layer plaque assay and expressed as plaque-forming units (PFU)/mL.[10] Polyvalent phages were characterized by TEM imaging, bacterial growth curve analysis, and plaque size with the details provided in Text S2.

Biofilm Cultivation for Phage Selection and Treatment. A dual-species biofilm (*P. aeruginosa* PAO1 and *E. coli* NDM-1) was established on 0.2 μm hydrophobic poly-(vinylidene difluoride (PVDF) membranes (Pall Corporation, USA). Briefly, bacteria harvested at the exponential phase were washed three times and diluted in phosphate-buffered saline (PBS) to an OD_{600} of 0.5. Then, 0.25 mL of *E. coli* and 0.25 mL of *P. aeruginosa* were inoculated in 5 mL of modified M63 medium[18] in a plastic petri dish (35 mm diameter ×10 mm height, VWR, USA) with membranes (1.5 cm×1.5 mm) immersed. Dishes were incubated at 37 °C with horizontal shaking at 50 rpm for 36 h. After gently washing away planktonic cells with PBS three times, the membrane biofilms were subject to phage adsorption and treatment.

A flow-through system with biofilm was constructed using two pieces of poly-(methyl methacrylate) plates (Goodfellow, USA) with a flow channel (1 cm in diameter and 10 cm in length) carved on the bottom plate (Figure S1). The plates were held together using screws with a silicone gasket to avoid

https://doi.org/10.1021/acs.est.2c06561
Environ. Sci. Technol. 2022, 56, 17177−17187

leakage. PVDF membranes carrying biofilms were cut into the proper size and securely loaded on the bottom of the channel to simulate the growth of biofilms on the pipe's inner surface.

Phage Display for Peptide Selection. The Ph.D.-7 Phage Display Peptide Library was used to screen peptides presenting high affinity to *P. aeruginosa* (Figure S2).[59] Briefly, 10^{11} phages from the library were mixed with 1 mL of fresh *P. aeruginosa* culture (stationary phase, diluted to OD_{600} = 0.1) for 1 h. Adsorbed phages were eluted from pelleted cells (by centrifugation) with glycine−HCl (pH = 2.2),[60−62] and then propagated in *E. coli* ER2738 culture followed by purification and PEG precipitation.

Both Ph.D.-7 and -12 Phage Display Peptide Libraries were used to screen the peptide against polyvalent phages (Figure S3). Polyvalent phages were immobilized on amine-functionalized CNCs using EDC and NHS as crosslinkers as described.[63] The calculation of immobilization density is provided in Text S3. Both CNCs and phage-coated CNCs were treated with 4% BSA to block vacant binding sites. The phage library (10^{11} phages in 1 mL PBS) was first incubated with 1 mg BSA-treated CNCs for 1 h, and then the unbound fraction was transferred to 1 mg phage-coated CNCs blocked with BSA. After 1 h of incubation, the particles were washed, followed by the elution and enrichment of bound phages.

The affinity screening processes mentioned above were repeated for four rounds to obtain phages exhibiting high affinity to *P. aeruginosa* cells or polyvalent phages. Plaque assays were performed on phages eluted from the fifth round. Ten well-separated plaques were subject to plaque PCR[64,65] to amplify the DNA segment coding peptides responsible for the specific affinity from the phage genome. PCR products were purified and sent to Genewiz (Azenta Life Sciences, USA) for sequencing. Details of PCR, plaque PCR, and DNA purification are provided in Text S4.

Construction of the Dual-Modified M13 Phage. M13SK phage was constructed for dual display of peptides on pIII and pVIII as previously described.[66] Briefly, whole plasmid mutagenesis was applied to delete restriction site *Pst*I from the "multiple cloning sites" area and introduce new restriction sites *Pst*I and *BamH*I into the pVIII gene of M13KE (A6250T, T1372A, and C1381G, respectively).[67] The resulting vector, M13SK, was amenable for pIII and pVIII display by direct ligation of synthesized oligonucleotides into the phage genome. Phage M13SK was propagated in *E. coli* ER2738 culture, followed by genome extraction and purification using a ZR plasmid Miniprep kit (ZYMO Research, USA).

For pIII display, oligonucleotides corresponding to the peptide specific for polyvalent phages were synthesized, annealed, and extended following the protocol of Ph.D. Peptide Display Cloning System (New England Biolabs, USA). Both the M13SK genome and the extended oligonucleotides were digested with *Eag*I and *Acc65*I and then ligated together using T4 ligase. Oligonucleotides encoding the *P. aeruginosa*-binding peptide were annealed, phosphorylated, and engineered into the *Pst*I and *BamH*I sites of the pVIII gene as previously reported.[28,67] Details of genetic modifications are provided in Text S5. The dual-modified M13SK genome was transformed into self-made electrocompetent *E. coli* ER2738 and subject to plaque assays. Well-separated plaques were picked, followed by phage DNA sequencing by Genewiz to confirm successful cloning.

Characterization of M13 Phage Modification. To evaluate the pVIII display, the adsorption efficiency of the dual-modified M13 phage on suspended *P. aeruginosa* cells was compared to the wildtype M13 phage and polyvalent phage. Briefly, 10^8 *P. aeruginosa* cells were incubated with 10^6 phages (pVIII-modified M13 phage, wildtype M13 phage or polyvalent phage, quantified by plaque assay) in 1 mL PBS for 10 min to allow phage attachment. Afterward, free phages were collected using centrifugation (5000 × *g*, 3 min) and quantified by plaque assay. Phage adsorption efficiency was determined as the number of adsorbed phages over total phages. To identify the phage binding site on the bacterial surface, *P. aeruginosa* cells with cell surface proteins removed (using proteinase K or SDS treatment) and cells with polysaccharides removed (using periodate or mutanolysin treatment) were both assayed for phage adsorption as previously reported.[68−70] The successful removal of bacterial surface proteins using this treatment protocol was verified by decreased adsorption of lambda phage (recognizing protein lamB on *E. coli* membrane[71]) to treated host bacteria (Figure S4). Details of phage adsorption assays and cell treatment are provided in Text S6. The adsorption of the pVIII-modified M13 phage on biofilms in flow-through systems was also compared with the wildtype M13 phage and polyvalent phage using our water distribution simulator. Briefly, the water channel embedded with PVDF membrane biofilms was filled with PBS, and phage suspension (10^5 PFU/mL in PBS) was injected into the channel by a syringe pump (Harvard Apparatus, USA) at a flow rate of 0.01 cm/s. Phage concentration in the effluent was determined by plaque assay to generate breakthrough curves.

The attachment of the dual-modified M13 phage (with peptides displayed on both pVIII and pIII) to immobilized polyvalent phages was visualized by fluorescent microscopic imaging to evaluate the pIII display. Specifically, polyvalent phages were coated on a CNC surface with vacant binding sites blocked following the same procedure as mentioned above. Dual-modified M13 phages (10^8) were incubated with 1 mg polyvalent phage-CNC complexes in 1 mL PBS with gentle revolving at 10 rpm for 10 min followed by gentle washing with PBS for six times. Immobilized PEBX was stained with DNA dye SYBR gold while the potentially attached M13 phage (not visualized by SYBR gold-staining) was labeled with the anti-M13 antibody followed by streptavidin-Texas Red treatment.[72] Phage-CNC complexes were observed under the Olympus IX-71 using a 40× objective. Polyvalent phages radiated green light when excited by a 488-nm laser line, while M13 phage antibodies radiated red light when excited by a 560-nm laser line.[18]

Biofilm Treatment with Phage Conjugates. Phage conjugates were prepared by mixing 10^{10} PFU/mL dual-modified M13 phages with 10^{10} PFU/mL polyvalent phages in PBS at 4 °C overnight with gentle revolving at 10 rpm, followed by a dilution of 500 times with PBS for biofilm treatment. Polyvalent phage only (10^6 PFU/mL in PBS), phage conjugates (the dual-modified M13 phage and polyvalent phage both at 10^6 PFU/mL in PBS), or PBS (as control) were passed through the water channel embedded with PVDF membrane biofilms at different rates (0−1 cm/s) for 30 min to allow phage attachment. Then, membrane biofilms were carefully taken out and gently washed with PBS for three times to remove free phages, followed by incubation in 5 mL PBS in a plastic petri dish for 4 h (at room

https://doi.org/10.1021/acs.est.2c06561
Environ. Sci. Technol. 2022, 56, 17177−17187

temperature without shaking) to allow phage infection, cell lysis, and further phage dispersion. Live bacteria in PBS were enumerated by plate counting to ascertain that a decrease of biofilm biomass after phage treatment was due to bacterial lysis rather than biomass dispersion.

For biofilm characterization, residual biofilms were separated from PVDF membranes for bacteria quantification or fluorescently stained for fluorescent microscopic analysis. The membranes holding residual biofilms were immersed in ice-cold 0.2% PBST followed by vigorous vertexing for 3 min and sonication at 40 kHz in a 4 °C bath sonicator (Branson Co., USA) for 10 min for biofilm separation and bacterial dispersion.[13] Viable bacteria were counted by plate assay and quantitative PCR (qPCR) targeting the 16S rRNA gene was performed to quantify the total bacteria.[73] The biofilm removal efficiency was determined as the relative difference between the treated biofilm and the control biofilm. As for fluorescent microscopic analysis, the residual biofilms on membranes were stained with SYTO 9 and propidium iodide (PI) following the instruction of the LIVE/DEAD BacLight kit. Membranes were then loaded on glass slides and observed under the Olympus IX-71 using a 20× objective. Live bacteria stained by STYO 9 radiate green light when excited by a 488-nm laser line, while dead bacteria stained by PI radiate red light when excited by a 560-nm laser line.[18] In addition, biofilm samples were collected for transcriptomic analysis on four quorum sensing (QS)-related genes (*sdiA*, *luxS*, *lasI*, and *lasR*), three EPS generation-related genes (*pslA*, *rhlA*, and *rcsF*), and two curli biosynthesis-related genes (*csgB* and *csgD*).[18] Details of qPCR and transcriptomic analysis are provided in Texts S7, S8 and Table S1.

Statistical Analyses. All of the experiments were performed independently in at least triplicate. Analysis of variance (ANOVA) and Student's *t*-test were used to determine statistical significance. Differences were considered to be significant at the 95% confidence level ($p < 0.05$). Fluorescent microscope images were analyzed using Image J.

RESULTS AND DISCUSSION

Polyvalent Lytic Phages with High Dispersity Were Isolated Using CNC-Bacteria Complexes. Bacteria were chemically conjugated with CNCs to enable rapid magnetic isolation of polyvalent phages from activated sludge. Specifically, amine-functionalized iron-carbide (Fe_3C-NH_2) CNCs were coated with vancomycin and PEG to enhance attachment to bacteria (Figure 1a). Surface modifications were confirmed by the corresponding change in elemental composition and physicochemical properties (e.g., hydrodynamic diameter and surface charge) (Figure S5 and Table S2). These surface modifications increased the affinity of CNCs to *P. aeruginosa* from 20 to 70% in PBS and from 5 to 43% in sludge (Figure 1b,c). Similarly, the affinity of modified CNCs to *E. coli* increased from 23 to 72% in PBS and from 6 to 40% in sludge (Figure 1b,c). The constructed CNC-bacteria complexes were then added to a phage pool extracted from activated sludge samples to separate appropriate polyvalent phages using a modified sequential multi-host approach. Phages capable of attaching to (and, therefore, infecting) the specific CNC-complexed bacteria were separated along with complexes using a magnet (Figure S6).

Phages of various morphologies (e.g., phage PEBX belonging to the *Siphoviridae* family, PEBY and PEBZ belonging to the *Myoviridae* family) were readily isolated

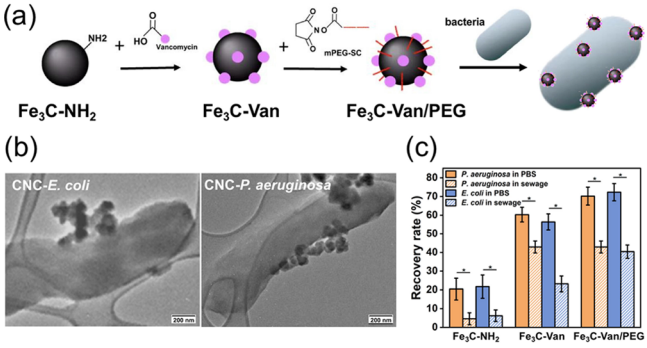

Figure 1. Magnetized bacteria for phage isolation. (a) Scheme of surface modified superparamagnetic CNCs for bacteria binding. (b) TEM imaging of *E. coli* and *P. aeruginosa* conjugated with modified superparamagnetic CNCs. (c) Bacteria recovery tests demonstrated enhanced bacteria affinity by CNCs after surface modification with vancomycin and PEG. Error bars in all figures represent standard deviation from triplicate experiments. Asterisks (*) indicate significant differences ($p < 0.05$) based on Student's *t*-test.

from activated sludge-derived phage pools (Figure 2a). Phages PEBX, PEBY, and PEBZ were all polyvalent and exhibited

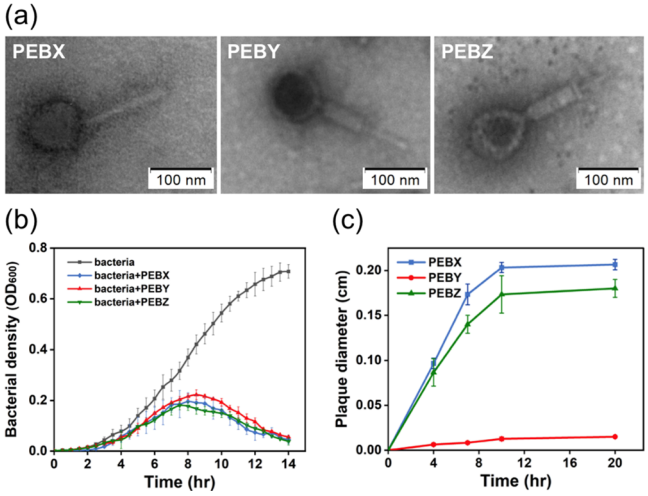

Figure 2. Polyvalent lytic phages isolated with magnetized bacterial hosts. (a) TEM images of polyvalent phages PEBX, PEBY, and PEBZ capable of infecting both *E. coli* and *P. aeruginosa*. (b) Bactericidal assays (growth curves) with a mixed culture of *E. coli* and *P. aeruginosa*. (c) Plaques sizes of phage PEBX, PEBY, and PEBZ on the mixed species lawn of *E. coli* and *P. aeruginosa*.

effective infection of both *P. aeruginosa* PAO1 and *E. coli* NDM-1 in suspended systems (Figure 2b). Additionally, plaque assays using stationary-phase *P. aeruginosa* and *E. coli* lawns showed that the diameters of clear plaques after 20-h incubation were 2.07 ± 0.06 mm for PEBX, 0.15 ± 0.01 mm for PEBY, and 1.80 ± 0.10 mm for PEBZ (Figures 2b and S7). This suggests that PEBX has relatively high dispersity and propagates efficiently in bacteria under resource-limited conditions, which are commonly observed in mature biofilms.[74] Thus, PEBX was selected for the construction of phage conjugates and biofilm eradication experiments.

Peptides with High Affinity for *P. aeruginosa* Were Displayed on M13 Major Coat Protein pVIII. For biofilm recognition and attachment, we chose not to target EPS protecting biofilm-dwelling bacteria since EPS structure and

https://doi.org/10.1021/acs.est.2c06561
Environ. Sci. Technol. 2022, 56, 17177−17187

components are highly variable and significantly influenced by surrounding conditions (e.g., temperature, oxygen, chemical pollutants, and nutrient availability) and biological factors (e.g., cell type, cell growth stage, and biofilm formation stage).[75−77] Rather, we targeted *P. aeruginosa*, a common opportunistic pathogen prevalent in DWDS,[29−31] which dominated this dual-species biofilm (and other multi-species biofilms in diverse environments)[41−46] because it has a relatively stable cell surface structure compared to the biofilm EPS. Three peptides presenting high affinity for *P. aeruginosa* cells in the stationary growth phase were obtained from a peptide library: YHLPVES, FSPGSVR, and ASWIAVR. Only peptide YHLPVES was successfully fused into pVIII for display (with additional amino acids at the 3′- ends) (Figure 3a,b), while the other two peptides failed, probably due to compromising pVIII structure and M13 viability.[78]

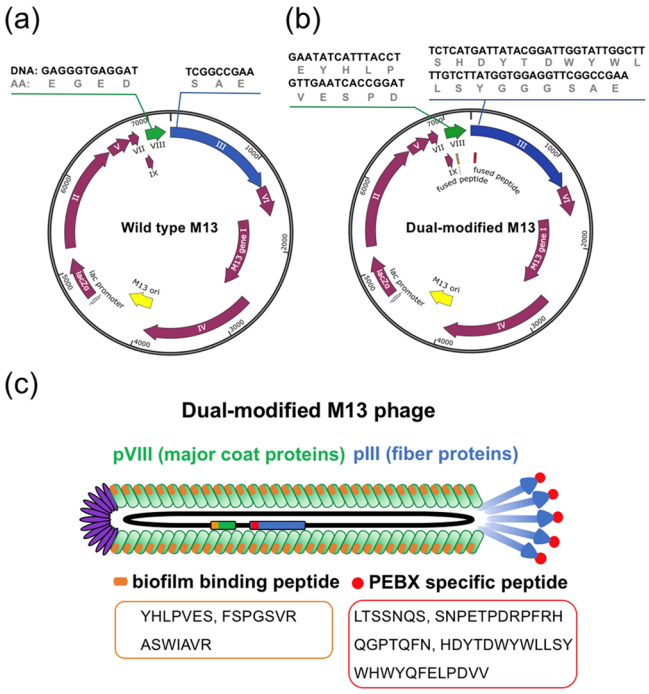

Figure 3. Scheme of dual modification of filamentous phage M13. (a) Genome map of wildtype M13 phage with sites suitable for foreign oligonucleotide insertion specified on genes coding major capsid protein (pVIII) and tail fibers (pIII). (b) Genome map of dual-modified M13 phage with oligonucleotide insertions. (c) pVIII was modified for *P. aeruginosa* biofilm recognition. Peptide candidates YHLPVES, FSPGSVR, and ASWIAVR were screened by phage display using *P. aeruginosa* as the target. pIII was modified for polyvalent phage PEBX conjugation. Peptide candidates LTSSNQS, SNPETPDRPFRH, QGPTQFN, HDYTDWYWLLSY, and WHWYQFELPDVV were screened by phage display using phage PEBX as the target.

The adsorption of the pVIII-modified M13 phage to *P. aeruginosa* suspended cells was assessed to determine the benefit of peptide fusion and display. The adsorption efficiency of the pVIII-modified M13 phage was 97 ± 1% after 10 min of phage-cell incubation, while that of PEBX was 28 ± 6% (Figure 4a). Wildtype M13 coliphage barely adsorbed to *P. aeruginosa* cells (at an efficiency of 5 ± 2%, Figure 4a), confirming that the greatly enhanced affinity resulted from the displayed peptide. Cell surface modification and phage adsorption assays revealed that the modified M13 phage binds to polysaccharide instead of proteins. The partial degradation of cell surface proteins (by SDS or proteinase K treatment[68]) did not significantly decrease the phage adsorption capacity of *P. aeruginosa* cells ($p > 0.05$) (Figure 4b), suggesting that the bacterial surface proteins were not associated with the adsorption of pVIII-modified M13 phage. In contrast, cells with polysaccharides partially degraded (by mutanolysin treatment to hydrolyze glycosidic bonds[68] or periodate treatment to degrade carbohydrates containing a 1,2-diol motif[69]) exhibited significantly reduced phage adsorption ($p < 0.05$), and adsorption efficiency was inversely related to polysaccharide degradation (i.e., periodate concentration) (Figure 4b). This corroborates that modified M13 binds to *P. aeruginosa* polysaccharides. Notably, polysaccharides are the major components of capsules or slimes of most gram-negative bacteria, including *P. aeruginosa*.[79,80] Moreover, polysaccharides comprise the outermost domain of the LPS molecule[81] that accounts for up to 75% of the gram-negative bacterial outer membrane surface.[82] Therefore, there is a higher possibility for polysaccharides rather than proteins to be adsorbed by peptide candidates during phage display.

Modified M13 phage also binds to dual-species biofilms with considerably higher efficiency than PEBX and wildtype M13 phage. Approximately 40% modified M13 phages were adsorbed to biofilms (with total live bacteria density ∼10^8 CFU/cm^2) in breakthrough studies with the drinking water pipe simulator, while only about 7% PEBX were adsorbed and no significant adsorption of wildtype M13 phage was observed (Figure 4c). Modified M13 phage displays ∼2700 copies of peptide YHLPVES along the phage capsid, which was approximately 2−3-log higher than the copy number of receptor-binding proteins identified in common phages.[83,84] Apparently, the high abundance of polysaccharide-binding sites along the major phage capsid enabled modified M13 to bind to *P. aeruginosa* cells in both planktonic and biofilm states with a considerably higher efficiency.

Peptides with High Affinity to PEBX Were Displayed on M13 Phage Fiber Proteins. Peptide YHLPVES would facilitate the binding of M13 to biofilms, but another peptide with high affinity for PEBX is also required to load the polyvalent phage cargo onto M13 for targeted delivery to biofilms. Five peptides with high affinity to PEBX phage were isolated with these sequences: HDYTDWYWLLSY, LTSSNQS, WHWYQFELPDVV, SNPETPDRPFRH, and QGPTQFN (Figure 3c). All were successfully fused and displayed in the fiber proteins (pIII) of pVIII-modified M13 phage using biosynthesis and genetic engineering strategies confirmed by gene sequencing (Figure 3b). The corresponding dual-modified M13 phages (Figure 3c) were named as III-1 to III-5 and their affinity for PEBX was examined by their attachment to PEBX immobilized onto CNC surfaces (approximately 10^8 PEBX/mg CNCs) as verified by fluorescent imaging (Figures 5a, S8 and S9). Specifically, PEBX-CNC complexes radiating green fluorescence (due to SYBR-gold stained PEBX) also exhibited red fluorescence carried by anti-M13 antibodies after incubation with dual-modified M13 phages, suggesting efficient attachment. In contrast, dual-modified M13 phage exhibited no affinity to the control CNCs without PEBX immobilized (Figure 5b), and pVIII-modified M13 phage did not adsorb to PEBX-CNC complexes (Figure 5c), confirming that the enhanced affinity resulted from peptide fusion into pIII.

https://doi.org/10.1021/acs.est.2c06561
Environ. Sci. Technol. 2022, 56, 17177−17187

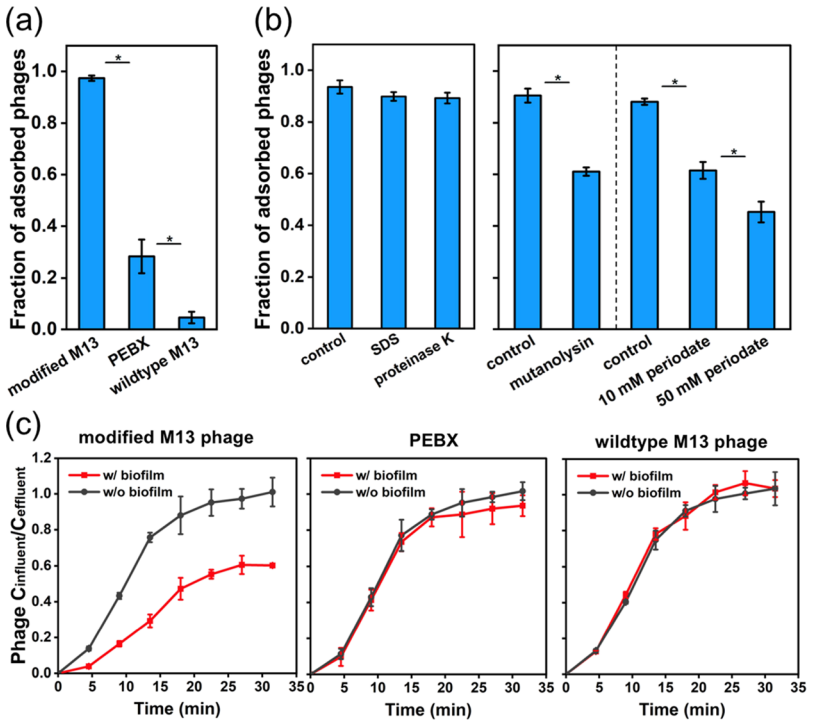

Figure 4. Enhanced affinity of modified M13 toward *P. aeruginosa*-dominated dual-species biofilm. (a) Modified M13 was more efficiently adsorbed by *P. aeruginosa* cells compared to phage PEBX or wildtype M13. (b) *P. aeruginosa* surface treated with protein disruptors did not affect modified phage M13 adsorption, while that treated with LPS disruptors significantly reduced bacterial adsorption toward modified phage M13. (c) Modified M13 was more efficiently adsorbed by *P. aeruginosa*-dominated dual-species biofilms compared to phage PEBX or wildtype M13. Asterisks (*) indicate significant differences ($p < 0.05$) based on Student's *t*-test.

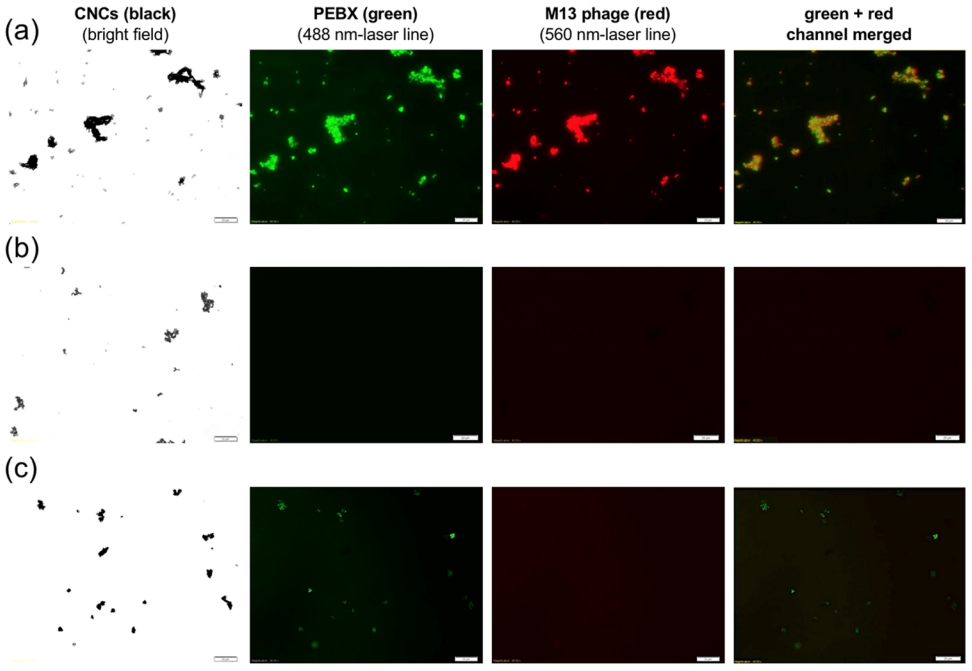

Figure 5. Fluorescent microscope analysis confirmed successful conjugation between dual-modified M13 phage and polyvalent phage PEBX due to peptide affinity. (a) PEBX-CNC complexes radiating green fluorescence (due to stained PEBX genome) also exhibited red fluorescence carried by anti-M13 antibodies due to the attachment of dual-modified M13 phage. (b) Dual-modified M13 phage did not attach to control CNCs without PEBX immobilized. (c) pVIII-modified M13 phage exhibited no affinity to PEBX-CNC complexes, suggesting that the enhanced affinity resulted from the peptide displayed on pIII. Scale bars represent 20 μm.

Theoretically, dual-modified M13 phage can be conjugated with PEBX without additional chemicals and biomaterials due to its specific peptide affinity. However, this phage conjugation might significantly compromise PEBX infectivity if M13 phage binds to the PEBX fiber tail and unintendedly blocks host receptor recognition and phage genome injection. Therefore,

https://doi.org/10.1021/acs.est.2c06561
Environ. Sci. Technol. 2022, 56, 17177−17187

the biofilm removal tests using the conjugates of PEBX and dual-modified M13 phage III-1 to III-5 were separately conducted to evaluate the effect of phage conjugation on biofilm recognition and eradication. Specifically, PVDF filtration membranes covered with dual-species biofilms were immersed in phage conjugates suspension (prepared by mixing 10^7 PFU/mL PEBX and 10^7 PFU/mL M13 phage) with residual biofilm characterized afterward.

Relative to the control groups without phage treatment, conjugates of PEBX with III-1 to III-5 resulted in 79 ± 5, 42 ± 13, 19 ± 5, 78 ± 4, and 61 ± 7% reduction of live biofilm bacteria, respectively, compared to only 19.1 ± 7.8% decrease for PEBX alone (Figure S10). In addition, 16S rRNA gene quantification showed 70 ± 8, 29 ± 12, 24 ± 10, 76 ± 4, and 69 ± 8% of biofilm reduction by the conjugates of PEBX and III-1 to III-5, respectively, versus 12 ± 7% for PEBX alone (Figure S9). The dramatically enhanced biofilm removal efficiency of PEBX conjugated with III-1 and III-4 suggests successful phage conjugation without significant interference of phage−host recognition and infection. Compared with III-1 and III-4, the conjugates of PEBX and III-2, III-3, or III-5 exhibited less effective biofilm removal, probably due to lower conjugation efficiency or hindering the ability of PEBX to recognize host receptors. Therefore, the conjugates of PEBX and dual-modified M13 phage III-1 (with the sequence as HDYTDWYWLLSY) were selected for biofilm control at flow-through conditions.

Phage Conjugates Enhanced Biofilm Removal Compared to PEBX Alone under Flow-Through Conditions. Hydrodynamic conditions, which affect phage-to-cell contact rate (initiating receptor recognition) and the stability of phage−cell pairs (to complete phage genome injection),[85] would influence the efficiency of phage treatment in DWDS. Specifically, under water stagnant conditions (i.e., flow rate = 0 cm/s, which is typical in water storage tanks[86] and some premise plumbing systems[87]), the PEBX-only treatment resulted in a 16 ± 12% decrease of live biofilm bacteria (determined by plate counting) and 12 ± 5% decrease of total bacteria (determined by 16S rRNA gene quantification) (Figure 6a). Phage conjugates further reduced biomass as live bacteria decreased by 77 ± 7% and total bacteria by 75 ± 11% (Figure 6a), suggesting more efficient biofilm removal due to enhanced phage delivery and higher infection rates.

Increased water flow rates promoted phage−bacteria contact events but also resulted in higher phage detachment due to the shearing force.[88] Compared to stagnant water conditions, PEBX treatment reduced live bacteria by 34 ± 6% and total biofilm bacteria by 28 ± 8% at a flow rate of 0.01 cm/s (Figure 6a). Conjugated phages consistently exhibited enhanced biofilm control efficiency compared to PEBX alone ($p < 0.05$) as live bacteria decreased by 84 ± 5% and total bacteria by 78 ± 4% (Figure 6a). Fluorescent microscopic imaging corroborated the decrease in biofilm coverage area after phage treatment (Figure S11). Specifically, biofilm coverage significantly decreased from 97 ± 2% (no-phage control) to 75 ± 5% by PEBX treatment ($p < 0.05$), and further to 14 ± 4% by conjugated phage treatment ($p < 0.05$) (Figure 6b). Due to phage infection and lysis of live bacteria, the phage-treated groups exhibited decreased ratios of live/dead cells and increased phage numbers (Figures 6b and S12). Biomass released from biofilms contained relatively low total numbers of live bacteria (10^2−10^4 cells) (Figure S13), suggesting efficient biofilm control as a result of bacterial lysis instead of

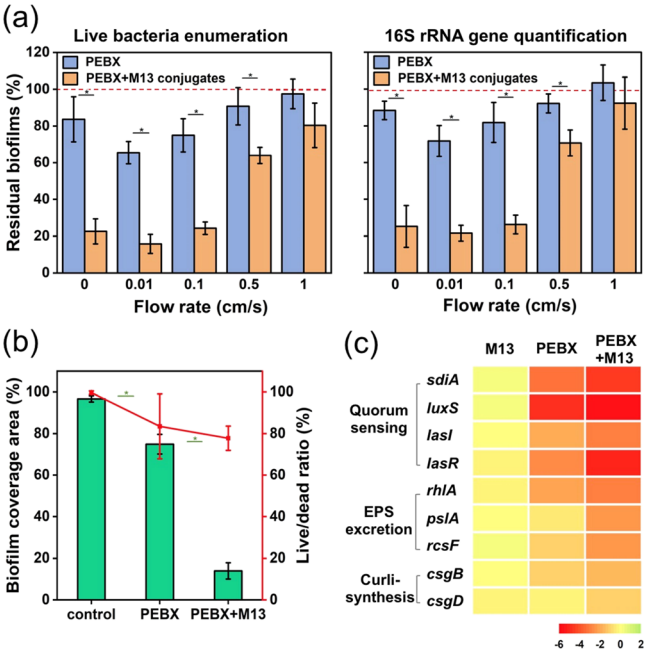

Figure 6. Enhanced control of biofilm bacteria using polyvalent phage PEBX conjugated with dual-modified phage M13. (a) Culture dependent and independent assays showed enhanced biofilm control by phage conjugates under continuous flow conditions. (b) Fraction of the remaining biofilm coverage area upon exposure to phages (no-phage as control) and live/dead cell ratio according to a fluorescent microscope analysis. (c) Transcriptomic analysis of genes associated with biofilm stability after biofilms treated with PEBX alone or phage conjugates. Fold changes are log2-transformed. Asterisks (*) indicate significant differences ($p < 0.05$) based on Student's *t*-test.

biomass dispersion. Extending the exposure time of biofilms to phage conjugates from 4 to 24 h resulted in a further decrease of biomass (i.e., from 84 ± 5 to 95 ± 2% for live bacteria and from 78 ± 4 to 96 ± 2% for total bacteria). In contrast, extended exposure to PEBX only did not significantly reduce biomass (Figure S14), probably reaching a steady state of phage−biofilm interactions.[20]

The biofilm removal efficiencies for both PEBX and conjugated phage treatments were negatively associated with flow rates ranging from 0.01 to 1 cm/s (Figure 6a), suggesting increased detachment rates due to higher shear force. Therefore, conjugated phage treatments are likely to be most effective for stagnant systems or those with low flow rates, which includes areas of drinking water systems that are most vulnerable to biofouling, such as storage tanks and building plumbing systems.[87,89] Phages could be supplemented through upstream access points (e.g., blow-off and hose bibbs).[90] Conjugating PEBX with dual-modified M13 phages resulted in significantly enhanced biofilm removal relative to the use of PEBX alone under these conditions. Moreover, neither PEBX nor dual-modified M13 phage exhibited significant adsorption to common materials for water tanks or pipes, including fiberglass, high density polyethylene, and polyvinyl chloride (Figure S15), which suggests efficient transport of phage conjugates to target biofilms without retention on tank or pipe surfaces.

Phage Conjugates Exhibited Extended Inhibition on Biofilms than PEBX Alone. Compared to treatment with only PEBX, phage conjugates exhibited more durable inhibition of biofilms. Using transcriptomic analysis, we

https://doi.org/10.1021/acs.est.2c06561
Environ. Sci. Technol. 2022, 56, 17177−17187

found that after 4-h treatment, PEBX downregulated QS related genes in both species (i.e., *sdiA* and *luxS* in *E. coli*;[91,92] *lasI* and *lasR* in *P. aeruginosa*[93]). This is conducive to reducing the secretion of signal molecules for bacterial communication, which may consequentially inhibit biofilm formation and regrowth.[94] PEBX conjugated with dual-modified M13 phage down-regulated QS secretion related genes to a greater extent than PEBX phage alone, which is consistent with the higher biofilm eradication efficiency than PEBX-only treatments (Figure 6a). Specifically, QS related genes were down-regulated by 8- to 48-fold upon exposure to phage conjugates relative to control tests without phages, while PEBX phage alone decreased their expression by 4- to 26-fold (Figure 6c).

Phage treatment also downregulated EPS synthesis genes (i.e., *rhlA*[95] and *pslA*[96] in *P. aeruginosa*; *rcsF*[97] in *E. coli*), with phage conjugates showing greater downregulation than PEBX alone. Specially, phage conjugate treatments down-regulated genes 4.8- to 7.2-fold while PEBX alone decreased expression 1.5- to 4.2-fold. The greater gene repression by phage conjugates resulted in a less dense biofilm structure and facilitated phage dispersion. The expression of curli-biosynthesis related genes, *csgB* (coding minor curlin subunit) and *csgD* (regulating CsgBA operon transcription)[98] in *E. coli*, respectively, decreased by 2.9- and 2.3-fold after phage conjugate treatment, and 2.0- and 1.8-fold after exposure to PEBX only (Figure 6c). This would suppress curli synthesis and impede biofilm regrowth as curli adhesion is important at the initial stages of biofilm formation.[99] Suppression of these biofilm-related genes upon exposure to phage PEBX at a low concentration (10^7 PFU/mL) was consistent with a previous report of a hormetic effect of lytic phages that stimulated biofilm growth when present at low titers.[18] In contrast, dual-modified M13 alone exerted no significant influence on gene expression, with an expression of the aforementioned seven genes ranging from 0.8- to 1.2-fold relative to control groups (Figure 6c).

Overall, conventional strategies to remove DWDS biofilms are either relatively inefficient or come with undesired side-effects. Polyvalent lytic phages (used as self-replicating green biocides) may serve as effective tools for biofilm eradication. However, insufficient phage exposure due to ineffective delivery might result in low efficacy of biofilm removal.[18] Here, we modified the M13 phage for enhanced targeting of biofilms in DWDS. This tunable approach could enable enhanced phage delivery and higher biofilm eradication efficacy to expand the scope of phage applications in flow-through systems. Notably, a bench-scale water pipe simulator was used for this proof-of-concept work, which encourages future studies with real DWDS and naturally developed biofilms, including larger temporal and special scales and a systematic consideration of critical environmental parameters (e.g., nutrient levels) that may affect biofilm growth, phage propagation, and decay rates.[100] Additionally, the M13 phage as a "shuttle" could be modified following a similar approach to display other specific peptides, and thus enable precise delivery of various cargos to address diverse environmental issues.

■ ASSOCIATED CONTENT

Supporting Information

The Supporting Information is available free of charge at https://pubs.acs.org/doi/10.1021/acs.est.2c06561.

Procedures for polyvalent phage isolation using CNCs, peptides screening using phage display, details of CNCs modification and characterization, transcriptomic analysis using RT-PCR and qPCR, phage adsorption tests toward biotic and abiotic agents, and results of long-term biofilm suppression using phage conjugates (PDF)

■ AUTHOR INFORMATION

Corresponding Authors

Pingfeng Yu − *College of Environmental and Resource Sciences, Zhejiang University, Hangzhou, Zhejiang 310058, China;* orcid.org/0000-0003-0402-773X; Email: yupf@zju.edu.cn

Pedro J.J. Alvarez − *Department of Civil and Environmental Engineering, Rice University, Houston, Texas 77005, United States;* orcid.org/0000-0002-6725-7199; Email: alvarez@rice.edu

Authors

Ruonan Sun − *Department of Civil and Environmental Engineering, Rice University, Houston, Texas 77005, United States*

Pengxiao Zuo − *Department of Civil and Environmental Engineering, Rice University, Houston, Texas 77005, United States*

Dino Villagrán − *Department of Chemistry and Biochemistry, The University of Texas at El Paso, El Paso, Texas 79968, United States;* orcid.org/0000-0002-5798-3584

Jacques Mathieu − *Department of Civil and Environmental Engineering, Rice University, Houston, Texas 77005, United States;* orcid.org/0000-0003-1776-8772

Complete contact information is available at: https://pubs.acs.org/10.1021/acs.est.2c06561

Notes

The authors declare no competing financial interest.

■ ACKNOWLEDGMENTS

This work was supported by National Natural Science Foundation of China (42277418), NSF ERC on Nanotechnology-Enabled Water Treatment (EEC-1449500) and the National Key Research and Development Program of China (2022YFC3704700). We thank Drs. Kuichang Zuo, Bo Zhang, and Zhuodong Yu for their help on reactor fabrication and biofilm characterization.

■ REFERENCES

(1) Flemming, H.-C.; Wingender, J. The biofilm matrix. *Nat. Rev. Microbiol.* **2010**, *8*, 623−633.

(2) Liu, S.; Gunawan, C.; Barraud, N.; Rice, S. A.; Harry, E. J.; Amal, R. Understanding, monitoring, and controlling biofilm growth in drinking water distribution systems. *Environ. Sci. Technol.* **2016**, *50*, 8954−8976.

(3) Wang, H.; Hu, C.; Hu, X.; Yang, M.; Qu, J. Effects of disinfectant and biofilm on the corrosion of cast iron pipes in a reclaimed water distribution system. *Water Res.* **2012**, *46*, 1070−1078.

(4) Douterelo, I.; Sharpe, R. L.; Boxall, J. B. Influence of hydraulic regimes on bacterial community structure and composition in an experimental drinking water distribution system. *Water Res.* **2013**, *47*, 503−516.

(5) Van der Wende, E.; Characklis, W. G.; Smith, D. Biofilms and bacterial drinking water quality. *Water Res.* **1989**, *23*, 1313−1322.

(6) Benedict, K. M.; Reses, H.; Vigar, M.; Roth, D. M.; Roberts, V. A.; Mattioli, M.; Cooley, L. A.; Hilborn, E. D.; Wade, T. J.; Fullerton,

K. E.; Yoder, J. S.; Hill, V. R. Surveillance for waterborne disease outbreaks associated with drinking water—United States, 2013−2014. *MMWR-Morb. Mortal. Wkly. Rep.* **2017**, *66*, 1216−1221.
(7) Beer, K. D.; Gargano, J. W.; Roberts, V. A.; Hill, V. R.; Garrison, L. E.; Kutty, P. K.; Hilborn, E. D.; Wade, T. J.; Fullerton, K. E.; Yoder, J. S. Surveillance for waterborne disease outbreaks associated with drinking water—United States, 2011−2012. *MMWR-Morb. Mortal. Wkly. Rep.* **2015**, *64*, 842−848.
(8) Yoder, J.; Roberts, V.; Craun, G. F.; Hill, V.; Hicks, L. A.; Alexander, N. T.; Radke, V.; Calderon, R. L.; Hlavsa, M. C.; Beach, M. J. Surveillance for waterborne disease and outbreaks associated with drinking water and water not intended for drinking–United States, 2005-2006. *MMWR Surveill Summ.* **2008**, *57*, 39−62.
(9) Liang, J. L.; Dziuban, E. J.; Craun, G. F.; Hill, V.; Moore, M. R.; Gelting, R. J.; Calderon, R. L.; Beach, M. J.; Roy, S. L. Surveillance for waterborne disease and outbreaks associated with drinking water and water not intended for drinking—United States, 2003−2004. *MMWR Surveill. Summ.* **2006**, *55*, 31−65.
(10) Yu, P.; Mathieu, J.; Yang, Y.; Alvarez, P. J. J. Suppression of enteric bacteria by bacteriophages: importance of phage polyvalence in the presence of soil bacteria. *Environ. Sci. Technol.* **2017**, *51*, 5270−5278.
(11) Motlagh, A. M.; Bhattacharjee, A. S.; Goel, R. Biofilm control with natural and genetically-modified phages. *World J. Microbiol. Biotechnol.* **2016**, *32*, 67.
(12) Pires, D. P.; Melo, L. D.; Boas, D. V.; Sillankorva, S.; Azeredo, J. Phage therapy as an alternative or complementary strategy to prevent and control biofilm-related infections. *Curr. Opin. Microbiol.* **2017**, *39*, 48−56.
(13) Lu, T. K.; Collins, J. J. Dispersing biofilms with engineered enzymatic bacteriophage. *Proc. Natl. Acad. Sci. U. S. A.* **2007**, *104*, 11197−11202.
(14) Mathieu, J.; Yu, P.; Zuo, P.; Da Silva, M. L. B.; Alvarez, P. J. J. Going viral: emerging opportunities for phage-based bacterial control in water treatment and reuse. *Acc. Chem. Res.* **2019**, *52*, 849−857.
(15) Yu, P.; Wang, Z.; Marcos-Hernandez, M.; Zuo, P.; Zhang, D.; Powell, C.; Pan, A. Y.; Villagrán, D.; Wong, M. S.; Alvarez, P. J. Bottom-up biofilm eradication using bacteriophage-loaded magnetic nanocomposites: a computational and experimental study. *Environ. Sci.-Nano* **2019**, *6*, 3539−3550.
(16) Yu, Z.; Schwarz, C.; Zhu, L.; Chen, L.; Shen, Y.; Yu, P. Hitchhiking behavior in bacteriophages facilitates phage infection and enhances carrier bacteria colonization. *Environ. Sci. Technol.* **2021**, *55*, 2462−2472.
(17) Wigginton, K. R.; Kohn, T. Virus disinfection mechanisms: the role of virus composition, structure, and function. *Curr. Opin. Virol.* **2012**, *2*, 84−89.
(18) Zhang, B.; Yu, P.; Wang, Z.; Alvarez, P. J. J. Hormetic promotion of biofilm growth by polyvalent bacteriophages at low concentrations. *Environ. Sci. Technol.* **2020**, *54*, 12358−12365.
(19) Gallet, R.; Shao, Y.; Wang, I.-N. High adsorption rate is detrimental to bacteriophage fitness in a biofilm-like environment. *BMC Evol. Biol.* **2009**, *9*, 241.
(20) Simmons, E. L.; Drescher, K.; Nadell, C. D.; Bucci, V. Phage mobility is a core determinant of phage−bacteria coexistence in biofilms. *ISME J.* **2018**, *12*, 531−543.
(21) Deutscher, S. L. Phage display in molecular imaging and diagnosis of cancer. *Chem. Rev.* **2010**, *110*, 3196−3211.
(22) Kehoe, J. W.; Kay, B. K. Filamentous phage display in the new millennium. *Chem. Rev.* **2005**, *105*, 4056−4072.
(23) Smith, G. P. Filamentous fusion phage: novel expression vectors that display cloned antigens on the virion surface. *Science* **1985**, *228*, 1315−1317.
(24) Kim, Y.-G.; Lee, C.-S.; Chung, W.-J.; Kim, E.-M.; Shin, D.-S.; Rhim, J.-H.; Lee, Y.-S.; Kim, B.-G.; Chung, J. Screening of LPS-specific peptides from a phage display library using epoxy beads. *Biochem. Biophys. Res. Commun.* **2005**, *329*, 312−317.
(25) Liu, P.; Han, L.; Wang, F.; Petrenko, V. A.; Liu, A. Gold nanoprobe functionalized with specific fusion protein selection from phage display and its application in rapid, selective and sensitive colorimetric biosensing of *Staphylococcus aureus*. *Biosens. Bioelectron.* **2016**, *82*, 195−203.
(26) Matsumoto, M.; Horiuchi, Y.; Yamamoto, A.; Ochiai, M.; Niwa, M.; Takagi, T.; Omi, H.; Kobayashi, T.; Suzuki, M.-M. Lipopolysaccaride-binding peptides obtained by phage display method. *J. Microbiol. Methods* **2010**, *82*, 54−58.
(27) Zourob, M.; Elwary, S.; Turner, A. P., *Principles of bacterial detection: biosensors, recognition receptors and microsystems*; Springer Science & Business Media: 2008.
(28) Wu, L.; Hong, X.; Luan, T.; Zhang, Y.; Li, L.; Huang, T.; Yan, X. Multiplexed detection of bacterial pathogens based on a cocktail of dual-modified phages. *Anal. Chim. Acta* **2021**, *1166*, No. 338596.
(29) Wang, H.; Masters, S.; Hong, Y.; Stallings, J.; Falkinham, J. O., III; Edwards, M. A.; Pruden, A. Effect of disinfectant, water age, and pipe material on occurrence and persistence of *Legionella*, *mycobacteria*, *Pseudomonas aeruginosa*, and two amoebas. *Environ. Sci. Technol.* **2012**, *46*, 11566−11574.
(30) Falkinham, J. O., III; Hilborn, E. D.; Arduino, M. J.; Pruden, A.; Edwards, M. A. Epidemiology and ecology of opportunistic premise plumbing pathogens: *Legionella pneumophila*, *Mycobacterium avium*, and *Pseudomonas aeruginosa*. *Environ. Health Perspect.* **2015**, *123*, 749−758.
(31) von Baum, H.; Bommer, M.; Forke, A.; Holz, J.; Frenz, P.; Wellinghausen, N. Is domestic tap water a risk for infections in neutropenic patients? *Infection* **2010**, *38*, 181−186.
(32) Huang, C. K.; Weerasekara, A.; Bond, P. L.; Weynberg, K. D.; Guo, J. Characterizing the premise plumbing microbiome in both water and biofilms of a 50-year-old building. *Sci. Total Environ.* **2021**, *798*, No. 149225.
(33) Lu, J.; Struewing, I.; Vereen, E.; Kirby, A. E.; Levy, K.; Moe, C.; Ashbolt, N. Molecular detection of Legionella spp. and their associations with *Mycobacterium* spp., *Pseudomonas aeruginosa* and amoeba hosts in a drinking water distribution system. *J. Appl. Microbiol.* **2016**, *120*, 509−521.
(34) Costa, D.; Bousseau, A.; Thevenot, S.; Dufour, X.; Laland, C.; Burucoa, C.; Castel, O. Nosocomial outbreak of *Pseudomonas aeruginosa* associated with a drinking water fountain. *J. Hosp. Infect.* **2015**, *91*, 271−274.
(35) Anaissie, E. J.; Penzak, S. R.; Dignani, M. C. The hospital water supply as a source of nosocomial infections: a plea for action. *Arch. Intern. Med.* **2002**, *162*, 1483−1492.
(36) Papapetropoulou, M.; Iliopoulou, J.; Rodopoulou, G.; Detorakis, J.; Paniara, O. Occurrence and antibiotic-resistance of *Pseudomonas species* isolated from drinking water in southern Greece. *J. Chemother.* **1994**, *6*, 111−116.
(37) Ashbolt, N. J. Environmental (saprozoic) pathogens of engineered water systems: understanding their ecology for risk assessment and management. *Pathogens* **2015**, *4*, 390−405.
(38) Trautmann, M.; Lepper, P. M.; Haller, M. Ecology of *Pseudomonas aeruginosa* in the intensive care unit and the evolving role of water outlets as a reservoir of the organism. *Am. J. Infect. Control* **2005**, *33*, S41−S49.
(39) De Victorica, J.; Galván, M. *Pseudomonas aeruginosa* as an indicator of health risk in water for human consumption. *Water Sci. Technol.* **2001**, *43*, 49−52.
(40) Wu, Q.; Ye, Y.; Li, F.; Zhang, J.; Guo, W. Prevalence and genetic characterization of *Pseudomonas aeruginosa* in drinking water in Guangdong Province of China. *LWT−Food Sci. Technol.* **2016**, *69*, 24−31.
(41) An, D.; Danhorn, T.; Fuqua, C.; Parsek, M. R. Quorum sensing and motility mediate interactions between *Pseudomonas aeruginosa* and *Agrobacterium tumefaciens* in biofilm cocultures. *Proc. Natl. Acad. Sci. U. S. A.* **2006**, *103*, 3828−3833.
(42) Cheng, Y.; Yam, J. K. H.; Cai, Z.; Ding, Y.; Zhang, L.-H.; Deng, Y.; Yang, L. Population dynamics and transcriptomic responses of *Pseudomonas aeruginosa* in a complex laboratory microbial community. *NPJ. Biofilms Microbiomes* **2019**, *5*, 1.

https://doi.org/10.1021/acs.est.2c06561
Environ. Sci. Technol. 2022, 56, 17177−17187

(43) Harrison, F.; Paul, J.; Massey, R. C.; Buckling, A. Interspecific competition and siderophore-mediated cooperation in *Pseudomonas aeruginosa*. *ISME J.* **2008**, *2*, 49−55.
(44) Hoffman, L. R.; Déziel, E.; d'Argenio, D. A.; Lépine, F.; Emerson, J.; McNamara, S.; Gibson, R. L.; Ramsey, B. W.; Miller, S. I. Selection for *Staphylococcus aureus* small-colony variants due to growth in the presence of *Pseudomonas aeruginosa*. *Proc. Natl. Acad. Sci. U. S. A.* **2006**, *103*, 19890−19895.
(45) Malic, S.; Hill, K. E.; Hayes, A.; Percival, S. L.; Thomas, D. W.; Williams, D. W. Detection and identification of specific bacteria in wound biofilms using peptide nucleic acid fluorescent in situ hybridization (PNA FISH). *Microbiology* **2009**, *155*, 2603−2611.
(46) Qu, L.; She, P.; Wang, Y.; Liu, F.; Zhang, D.; Chen, L.; Luo, Z.; Xu, H.; Qi, Y.; Wu, Y. Effects of norspermidine on *Pseudomonas aeruginosa* biofilm formation and eradication. *Microbiology* **2016**, *5*, 402−412.
(47) Murray, T. S.; Kazmierczak, B. I. *Pseudomonas aeruginosa* exhibits sliding motility in the absence of type IV pili and flagella. *J. Bacteriol.* **2008**, *190*, 2700−2708.
(48) Wood, T. E.; Howard, S. A.; Förster, A.; Nolan, L. M.; Manoli, E.; Bullen, N. P.; Yau, H. C.; Hachani, A.; Hayward, R. D.; Whitney, J. C.; Vollmer, W.; Freemont, P. S.; Filloux, A. The *Pseudomonas aeruginosa* T6SS delivers a periplasmic toxin that disrupts bacterial cell morphology. *Cell Rep.* **2019**, *29*, 187−201.e7.
(49) Morales, D. K.; Jacobs, N. J.; Rajamani, S.; Krishnamurthy, M.; Cubillos-Ruiz, J. R.; Hogan, D. A. Antifungal mechanisms by which a novel *Pseudomonas aeruginosa* phenazine toxin kills *Candida albicans* in biofilms. *Mol. Microbiol.* **2010**, *78*, 1379−1392.
(50) Ghequire, M. G.; De Mot, R. Ribosomally encoded antibacterial proteins and peptides from *Pseudomonas*. *FEMS Microbiol. Rev.* **2014**, *38*, 523−568.
(51) Madsen, J. S.; Lin, Y.-C.; Squyres, G. R.; Price-Whelan, A.; de Santiago Torio, A.; Song, A.; Cornell, W. C.; Sørensen, S. J.; Xavier, J. B.; Dietrich, L. E. Facultative control of matrix production optimizes competitive fitness in *Pseudomonas aeruginosa* PA14 biofilm models. *Appl. Environ. Microbiol.* **2015**, *81*, 8414−8426.
(52) Nadell, C. D.; Ricaurte, D.; Yan, J.; Drescher, K.; Bassler, B. L. Flow environment and matrix structure interact to determine spatial competition in *Pseudomonas aeruginosa* biofilms. *Elife* **2017**, *6*, No. e21855.
(53) Denamur, E.; Clermont, O.; Bonacorsi, S.; Gordon, D. The population genetics of pathogenic *Escherichia coli*. *Nat. Rev. Microbiol.* **2021**, *19*, 37−54.
(54) Abberton, C. L.; Bereschenko, L.; van der Wielen, P. W. J. J.; Smith, C. J. Survival, biofilm formation, and growth potential of environmental and enteric *Escherichia coli* strains in drinking water microcosms. *Appl. Environ. Microbiol.* **2016**, *82*, 5320−5331.
(55) Zhong, D.; Zhuo, Y.; Feng, Y.; Yang, X. Employing carbon dots modified with vancomycin for assaying Gram-positive bacteria like *Staphylococcus aureus*. *Biosens. Bioelectron.* **2015**, *74*, 546−553.
(56) Zhu, M.; Liu, W.; Liu, H.; Liao, Y.; Wei, J.; Zhou, X.; Xing, D. Construction of Fe_3O_4/vancomycin/PEG magnetic nanocarrier for highly efficient pathogen enrichment and gene sensing. *ACS Appl. Mater. Interfaces* **2015**, *7*, 12873−12881.
(57) Ross, A.; Ward, S.; Hyman, P. More is better: selecting for broad host range bacteriophages. *Front. Microbiol.* **2016**, *7*, 1352.
(58) Yu, P.; Mathieu, J.; Li, M.; Dai, Z.; Alvarez, P. J. Isolation of polyvalent bacteriophages by sequential multiple-host approaches. *Appl. Environ. Microbiol.* **2015**, *82*, 808−815.
(59) Carnazza, S.; Foti, C.; Gioffrè, G.; Felici, F.; Guglielmino, S. Specific and selective probes for *Pseudomonas aeruginosa* from phage-displayed random peptide libraries. *Biosens. Bioelectron.* **2008**, *23*, 1137−1144.
(60) Linse, S.; Sormanni, P.; O'Connell, D. J. An aggregation inhibitor specific to oligomeric intermediates of Aβ42 derived from phage display libraries of stable, small proteins. *Proc. Natl. Acad. Sci. U. S. A.* **2022**, *119*, No. e2121966119.
(61) Dieltjens, T.; Willems, B.; Coppens, S.; Van Nieuwenhove, L.; Humbert, M.; Dietrich, U.; Heyndrickx, L.; Vanham, G.; Janssens, W. Unravelling the antigenic landscape of the HIV-1 subtype A envelope of an individual with broad cross-neutralizing antibodies using phage display peptide libraries. *J. Virol. Methods* **2010**, *169*, 95−102.
(62) Jaworski, J. W.; Raorane, D.; Huh, J. H.; Majumdar, A.; Lee, S.-W. Evolutionary screening of biomimetic coatings for selective detection of explosives. *Langmuir* **2008**, *24*, 4938−4943.
(63) Li, L.-L.; Yu, P.; Wang, X.; Yu, S.-S.; Mathieu, J.; Yu, H.-Q.; Alvarez, P. J. Enhanced biofilm penetration for microbial control by polyvalent phages conjugated with magnetic colloidal nanoparticle clusters (CNCs). *Environ. Sci.: Nano* **2017**, *4*, 1817−1826.
(64) Sørensen, M. C. H.; Vitt, A.; Neve, H.; Soverini, M.; Ahern, S. J.; Klumpp, J.; Brøndsted, L. Campylobacter phages use hypermutable polyG tracts to create phenotypic diversity and evade bacterial resistance. *Cell Rep.* **2021**, *35*, No. 109214.
(65) Born, Y.; Knecht, L. E.; Eigenmann, M.; Bolliger, M.; Klumpp, J.; Fieseler, L. A major-capsid-protein-based multiplex PCR assay for rapid identification of selected virulent bacteriophage types. *Arch. Virol.* **2019**, *164*, 819−830.
(66) Hess, G. T.; Cragnolini, J. J.; Popp, M. W.; Allen, M. A.; Dougan, S. K.; Spooner, E.; Ploegh, H. L.; Belcher, A. M.; Guimaraes, C. P. M13 bacteriophage display framework that allows sortase-mediated modification of surface-accessible phage proteins. *Bioconjugate Chem.* **2012**, *23*, 1478−1487.
(67) Ghosh, D.; Kohli, A. G.; Moser, F.; Endy, D.; Belcher, A. M. Refactored M13 bacteriophage as a platform for tumor cell imaging and drug delivery. *ACS Synth. Biol.* **2012**, *1*, 576−582.
(68) Binetti, A. G.; Quiberoni, A.; Reinheimer, J. A. Phage adsorption to *Streptococcus thermophilus*. Influence of environmental factors and characterization of cell-receptors. *Food Res. Int.* **2002**, *35*, 73−83.
(69) Kiljunen, S.; Datta, N.; Dentovskaya, S. V.; Anisimov, A. P.; Knirel, Y. A.; Bengoechea, J. A.; Holst, O.; Skurnik, M. Identification of the lipopolysaccharide core of *Yersinia pestis* and *Yersinia pseudotuberculosis* as the receptor for bacteriophage φA1122. *J. Bacteriol.* **2011**, *193*, 4963−4972.
(70) Gong, Q.; Wang, X.; Huang, H.; Sun, Y.; Qian, X.; Xue, F.; Ren, J.; Dai, J.; Tang, F. Novel host recognition mechanism of the K1 capsule-specific phage of *Escherichia coli*: capsular polysaccharide as the first receptor and lipopolysaccharide as the secondary receptor. *J. Virol.* **2021**, *95*, No. e0092021.
(71) Chatterjee, S.; Rothenberg, E. Interaction of bacteriophage λ with its *E. coli* receptor, LamB. *Viruses* **2012**, *4*, 3162−3178.
(72) Poul, M.-A.; Marks, J. D. Targeted gene delivery to mammalian cells by filamentous bacteriophage. *J. Mol. Biol.* **1999**, *288*, 203−211.
(73) Schloss, P. D.; Hay, A. G.; Wilson, D. B.; Gossett, J. M.; Walker, L. P. Quantifying bacterial population dynamics in compost using 16S rRNA gene probes. *Appl. Microbiol. Biotechnol.* **2005**, *66*, 457−463.
(74) Stewart, P. S.; Franklin, M. J. Physiological heterogeneity in biofilms. *Nat. Rev. Microbiol.* **2008**, *6*, 199−210.
(75) Loustau, E.; Leflaive, J.; Boscus, C.; Amalric, Q.; Ferriol, J.; Oleinikova, O.; Pokrovsky, O. S.; Girbal-Neuhauser, E.; Rols, J.-L. The response of extracellular polymeric substances production by phototrophic biofilms to a sequential disturbance strongly depends on environmental conditions. *Front. Microbiol.* **2021**, *12*, No. 742027.
(76) Toyofuku, M.; Inaba, T.; Kiyokawa, T.; Obana, N.; Yawata, Y.; Nomura, N. Environmental factors that shape biofilm formation. *Biosci., Biotechnol., Biochem.* **2016**, *80*, 7−12.
(77) Yesankar, P. J.; Qureshi, A.; Purohit, H. J., Biofilm-mediated biodegradation of hydrophobic organic compounds in the presence of metals as co-contaminants. In *Microbial Biodegradation and Bioremediation*; Elsevier: 2022; 441−460.
(78) Li, Z.; Koch, H.; Dübel, S. Mutations in the N-terminus of the major coat protein (pVIII, gp8) of filamentous bacteriophage affect infectivity. *Microb. Physiol.* **2003**, *6*, 57−66.
(79) Bazaka, K.; Crawford, R. J.; Nazarenko, E. L.; Ivanova, E. P. Bacterial extracellular polysaccharides. *Adv. Exp. Med. Biol.* **2011**, *715*, 213−226.

https://doi.org/10.1021/acs.est.2c06561
Environ. Sci. Technol. 2022, 56, 17177−17187

(80) Evans, L. R.; Linker, A. Production and characterization of the slime polysaccharide of *Pseudomonas aeruginosa*. *J. Bacteriol.* **1973**, *116*, 915−924.
(81) King, J. D.; Vinogradov, E.; Tran, V.; Lam, J. S. Biosynthesis of uronamide sugars in *Pseudomonas aeruginosa* O6 and *Escherichia coli* O121 O antigens. *Environ. Microbiol.* **2010**, *12*, 1531−1544.
(82) Raetz, C. R. H.; Whitfield, C. Lipopolysaccharide endotoxins. *Annu. Rev. Biochem.* **2002**, *71*, 635−700.
(83) Nobrega, F. L.; Vlot, M.; de Jonge, P. A.; Dreesens, L. L.; Beaumont, H. J.; Lavigne, R.; Dutilh, B. E.; Brouns, S. J. Targeting mechanisms of tailed bacteriophages. *Nat. Rev. Microbiol.* **2018**, *16*, 760−773.
(84) Flayhan, A.; Wien, F.; Paternostre, M.; Boulanger, P.; Breyton, C. New insights into pb5, the receptor binding protein of bacteriophage T5, and its interaction with its *Escherichia coli* receptor FhuA. *Biochimie* **2012**, *94*, 1982−1989.
(85) Sun, R.; Yu, P.; Zuo, P.; Alvarez, P. J. Bacterial concentrations and water turbulence influence the importance of conjugation versus phage-mediated antibiotic resistance gene transfer in suspended growth systems. *ACS Environ. Au* **2021**, *2*, 156−165.
(86) Alizadeh Fard, M.; Barkdoll, B. D. Stagnation reduction in drinking water storage tanks through internal piping with implications for water quality improvement. *J. Hydraul. Eng.* **2018**, *144*, No. 05018004.
(87) Falkinham, J. O., III; Pruden, A.; Edwards, M. Opportunistic premise plumbing pathogens: increasingly important pathogens in drinking water. *Pathogens* **2015**, *4*, 373−386.
(88) Murray, A. G.; Jackson, G. A. Viral dynamics - a model of the effects of size, shape, motion and abundance of single-celled planktonic organisms and other particles. *Mar. Ecol. Prog. Ser.* **1992**, *89*, 103−116.
(89) Bachmann, R. T.; Edyvean, R. G. J. Biofouling: an historic and contemporary review of its causes, consequences and control in drinking water distribution systems. *Biofilms* **2005**, *2*, 197−227.
(90) Rhoads, W. J.; Garner, E.; Ji, P.; Zhu, N.; Parks, J.; Schwake, D. O.; Pruden, A.; Edwards, M. A. Distribution system operational deficiencies coincide with reported *Legionnaires'* disease clusters in Flint, Michigan. *Environ. Sci. Technol.* **2017**, *51*, 11986−11995.
(91) Lee, J.; Maeda, T.; Hong, S. H.; Wood, T. K. Reconfiguring the quorum-sensing regulator SdiA of *Escherichia coli* to control biofilm formation via indole and *N*-acylhomoserine lactones. *Appl. Environ. Microbiol.* **2009**, *75*, 1703−1716.
(92) Walters, M.; Sperandio, V. Quorum sensing in *Escherichia coli* and *Salmonella*. *Int. J. Med. Microbiol.* **2006**, *296*, 125−131.
(93) Sakuragi, Y.; Kolter, R. Quorum-sensing regulation of the biofilm matrix genes (*pel*) of *Pseudomonas aeruginosa*. *J. Bacteriol.* **2007**, *189*, 5383−5386.
(94) McDougald, D.; Rice, S. A.; Barraud, N.; Steinberg, P. D.; Kjelleberg, S. Should we stay or should we go: mechanisms and ecological consequences for biofilm dispersal. *Nat. Rev. Microbiol.* **2012**, *10*, 39−50.
(95) Wang, S.; Yu, S.; Zhang, Z.; Wei, Q.; Yan, L.; Ai, G.; Liu, H.; Ma, L. Z. Coordination of swarming motility, biosurfactant synthesis, and biofilm matrix exopolysaccharide production in *Pseudomonas aeruginosa*. *Appl. Environ. Microbiol.* **2014**, *80*, 6724−6732.
(96) Karatan, E.; Watnick, P. Signals, regulatory networks, and materials that build and break bacterial biofilms. *Microbiol. Mol. Biol. Rev.* **2009**, *73*, 310−347.
(97) Castanié-Cornet, M.-P.; Cam, K.; Jacq, A. RcsF is an outer membrane lipoprotein involved in the RcsCDB phosphorelay signaling pathway in *Escherichia coli*. *J. Bacteriol.* **2006**, *188*, 4264−4270.
(98) Wang, X.; Zhou, Y.; Ren, J.-J.; Hammer, N. D.; Chapman, M. R. Gatekeeper residues in the major curlin subunit modulate bacterial amyloid fiber biogenesis. *Proc. Natl. Acad. Sci. U. S. A.* **2010**, *107*, 163−168.
(99) Barnhart, M. M.; Chapman, M. R. Curli biogenesis and function. *Annu. Rev. Microbiol.* **2006**, *60*, 131−147.
(100) Bryan, D.; El-Shibiny, A.; Hobbs, Z.; Porter, J.; Kutter, E. M. Bacteriophage T4 infection of stationary phase *E. coli*: life after log from a phage perspective. *Front. Microbiol.* **2016**, *7*, 1391.

https://doi.org/10.1021/acs.est.2c06561
Environ. Sci. Technol. 2022, 56, 17177−17187